Gradual localization of Ni 3*d* states in $LaNiO_3$ ultrathin films induced by dimensional crossover

Enju Sakai,[1,2] Masatomo Tamamitsu,[2] Kohei Yoshimatsu,[2] Satoshi Okamoto,[3] Koji Horiba,[2,4] Masaharu Oshima,[2,4] and Hiroshi Kumigashira[1,2,5,*]

[1]*Photon Factory and Condensed Matter Research Center, Institute of Materials Structure Science, High Energy Accelerator Research Organization, Tsukuba, Ibaraki 305-0801, Japan*

[2]*Department of Applied Chemistry, University of Tokyo, Bunkyo-ku, Tokyo 113-8656, Japan*

[3]*Materials Science and Technology Division, Oak Ridge National Laboratory, Oak Ridge, Tennessee 37831, USA*

[4]*Synchrotron Radiation Research Organization, University of Tokyo, Bunkyo-ku, Tokyo 113-8656, Japan*

[5]*PRESTO, Japan Science and Technology Agency, Kawaguchi, Saitama 332-0012, Japan*

(Received 31 July 2012; revised manuscript received 29 January 2013; published 20 February 2013)

In situ photoemission spectroscopy and x-ray absorption spectroscopy (XAS) have been performed on $LaNiO_3$ (LNO) ultrathin films grown on $LaAlO_3$ substrates to investigate the origin of the thickness-dependent metal-insulator transition (MIT). With decreasing film thickness, the progressive weakening of a quasiparticle peak at the Fermi level (E_F) occurs below 10 monolayer (ML), and the further depletion of spectral weight at E_F leads to pseudogap behavior at 3–6 ML. The pseudogap finally evolves into a full gap, indicating that the thickness-dependent MIT takes place at a critical film thickness of 2–3 ML. The observed spectral behavior is in line with the transport properties of LNO ultrathin films. The thickness dependence of the spectral intensity is compared with realistic multiorbital dynamical mean-field theory. The experimental spectral function was found to depend on the film thickness more strongly than the theoretical one for thinner systems, indicating that the thickness-dependent MIT in LNO is caused by the crossover from three to two dimensions, during which the spatial correlations are progressively enhanced. The XAS results suggest that a charge disproportionate state is strongly suppressed in LNO ultrathin films plausibly as a result of epitaxial strain from the substrates. These results strongly suggest that a novel insulating state is realized in LNO films at a thin limit.

DOI: 10.1103/PhysRevB.87.075132 PACS number(s): 71.30.+h, 79.60.−i, 73.20.−r, 73.50.−h

I. INTRODUCTION

Immediately after the prediction of the similarity between the electronic structures of the $LaNiO_3/LaAlO_3$ superlattice and those of high-T_c cuprates,[1–3] a number of experimental efforts were devoted to exploring possible high-T_c superconductivity in heterostructures based on $LaNiO_3$ (LNO).[4–8] The theory predicted the emergence of two-dimensional electron liquid states in the LNO layer as a result of the quantum confinement of Ni 3*d* electrons.[2,3] The resultant $d_{x^2-y^2}$ orbital ordering produces a single Fermi surface resembling that in the cuprates. However, almost all experiments reported that the heterostructures or ultrathin films underwent the transition from metal to insulator at a critical LNO-layer thickness of 3–5 monolayer (ML),[4–8] strongly suggesting the intrinsic insulating ground states of the LNO layer at a thin limit.

Despite intensive theoretical and experimental studies,[6–12] the origin of the thickness-dependent metal-insulator transition (MIT) in the LNO layer remains unclear, and a large number of discussions exist on the fundamental origin of the insulating ground states of LNO ultrathin films. One of the scenarios proposed for describing the physics of the insulating ground states is "dimensional-crossover-driven MIT."[6,13] According to this scenario, a decrease in the layer thickness of LNO causes a reduction in the effective bandwidth W owing to the prevention of charge transfer at the interface and the surface. The resultant reduction in W from a three-dimensional thick film (layer) to a two-dimensional ultrathin film (layer) may drive MIT in an LNO film (a superlattice based on LNO) at a thin limit.

On the other hand, it is well known that rare-earth nickel perovskites ($RNiO_3$, where R = rare earth) exhibit insulating ground states as a result of temperature-driven MIT for most rare earth ions except La.[14] The transition temperature increases with decreasing size of the R ion, suggesting that the gap opening would be due to a smaller Ni-O-Ni superexchange angle, leading to a reduction in W. The similar "bandwidth reduction" scenario is applicable to the insulating ground states in LNO ultrathin films:[12,15,16] The possible octahedral tilts and rotations due to the structural influence from substrates make a Ni-O-Ni super exchange angle smaller at an interface region, and the resultant reduction in W may cause the insulating ground states in LNO film at a thin limit. However, recent studies have revealed that charge disproportionation ($2Ni^{3+} \rightarrow Ni^{3+\delta} + Ni^{3-\delta}$) is also responsible for the insulating ground states in all the members of $RNiO_3$.[17,18] The first-order temperature-driven MIT accompanied by a structural change from orthorhombic to monoclinic phase is characteristic of the MIT in $RNiO_3$.

In contrast, the thickness-dependent MIT in LNO is marked by gradually localized behavior with a reduction in the LNO layer thicknesses. The LNO layer transforms from metallic to insulating states through intermediate localized states (bad metal or variable-range-hopping (VRH) regimes) with decreasing LNO layers.[4–8] The gradually localized behavior in transport properties of LNO contrasts sharply with the temperature-driven MIT in other $RNiO_3$,[14] suggesting the absence or strong suppression of the charge-disproportionate states in insulating states of LNO layers plausibly as a result of epitaxial strain.

To understand the origin of the thickness-dependent MIT in LNO as well as the insulating ground states at a thin limit, it is crucial to obtain information on how the electronic structures

change as a function of layer thickness, especially information on the possible evolution of charge disproportionation across the MIT, which is characteristic of insulating states of bulk $R\mathrm{NiO_3}$.

In this study, we address these questions through *in situ* photoemission spectroscopy (PES) and x-ray absorption spectroscopy (XAS) measurements on LNO ultrathin films grown on $\mathrm{LaAlO_3}$ (LAO) substrates with varying film thickness. In the PES spectra near the Fermi level (E_F), the thickness-dependent MIT was clearly observed at a critical film thickness of 2–3 ML through the pseudogap behavior at a thickness of 3–6 ML. These critical thicknesses were consistent with previously reported transport measurements.[4–8] The weakening of a quasiparticle peak and subsequent formation of a pseudogap at E_F are consistent with an intermediate weakly localized state in this film thickness, as observed in the transport measurements. The observed spectral changes in the PES are compared with the layer extension of a multiorbital dynamical mean-field theory (DMFT) calculation. While the spectral intensity is decreased with decreasing film thickness, a "Mott" insulating state is not stabilized down to the thinnest system even with a relatively large U. On the other hand, the experimental behavior is closer to a phenomenological cellular DMFT (CDMFT) calculation including short-range correlations. These results indicate that dimensional crossover from three to two dimensions[6] is the key physics for controlling the thickness-dependent MIT in LNO ultrathin films and for stabilizing an insulating state with short-range correlations or some form of long-range ordering in the thinnest system. From the XAS measurements on the Ni L edge, it is suggested that the charge disproportionation as observed in other $R\mathrm{NiO_3}$ family is strongly suppressed in the insulating states of LNO ultrathin films plausibly as a result of epitaxial strain. These results suggest that the novel intrinsic insulating ground states are realized in LNO ultrathin films where the charge disproportionation has minor contribution to the MIT.

II. EXPERIMENTAL

Digitally controlled LNO ultrathin films were grown on the (001) surface (in terms of the pseudocubic description) of an LAO substrate in a laser molecular-beam epitaxy chamber connected to a photoemission system at BL2C of the Photon Factory, KEK.[19] During deposition, the substrate temperature was maintained at 450 °C under an oxygen pressure of 10^{-3} Torr. The film thickness was precisely controlled on the atomic scale by monitoring the intensity oscillation of reflection high-energy electron diffraction (RHEED) as shown in Fig. 1(a). The LNO thin films were subsequently annealed at 400 °C for 45 min in oxygen at atmospheric pressure to remove oxygen vacancies. The absence of oxygen vacancies was also confirmed by *in situ* O 1*s* XAS measurements.[20,21] It should be noted that the physical properties of the films are almost the same as those of published data, which will be discussed in detail later, although the deposition condition in the present study is relatively lower compared to previous reports (450–750 °C and 0.01–0.4 Torr).[9,10,21,22] The good agreements indicate that the high quality LNO films are obtained in the present studies irrespective of the difference in growth conditions. The PES measurements were performed *in situ* using a VG-Scienta SES-2002 analyzer with a total energy resolution of 120 meV at room temperature. The XAS spectra were also measured *in situ* in the total electron-yield mode. The surface morphology of the measured films was analyzed by *ex situ* atomic force microscopy (AFM) in air. The crystal structure was characterized by cross-sectional transmission electron microscopy (TEM) and the synchrotron based x-ray diffraction (XRD) measurements performed at BL4C of the Photon Factory, KEK. The electrical resistivity of the films was measured by the four-probe method.

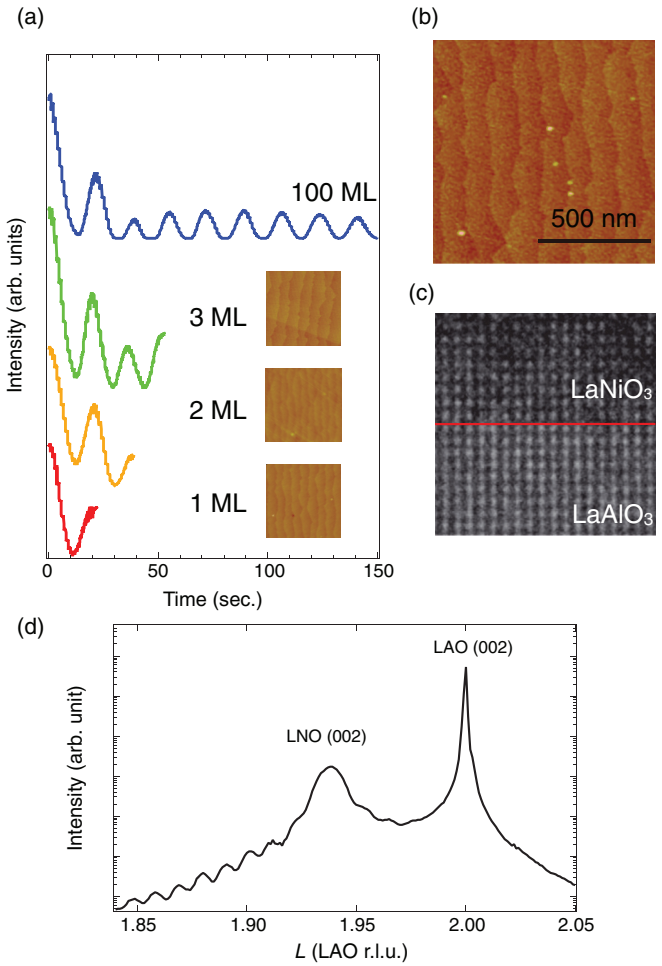

FIG. 1. (Color online) Characterizations of $\mathrm{LaNiO_3}$ films grown onto $\mathrm{LaAlO_3}$ substrates: (a) Typical RHEED intensity oscillations and corresponding AFM images (scan area $1 \times 1\ \mu\mathrm{m}^2$). (b) A typical AFM image of LNO films (100 ML). (c) Cross-sectional TEM image of the interface between LNO and LAO. A line indicates the interface between the two. (d) Synchrotron based XRD pattern along ($00L$) scan around the (002) reflections of an LNO film (100 ML) and an LAO substrate.

III. RESULTS AND DISCUSSION

Before discussing spectroscopic results, we provide evidence for the fact that the prepared LNO films have atomically flat surfaces and chemically abrupt LNO/LAO interfaces. These features comprise a precondition to the present thickness dependent study, and the evidence guarantees that the precondition is fulfilled. Figures 1(b)–1(d) show the characterizations

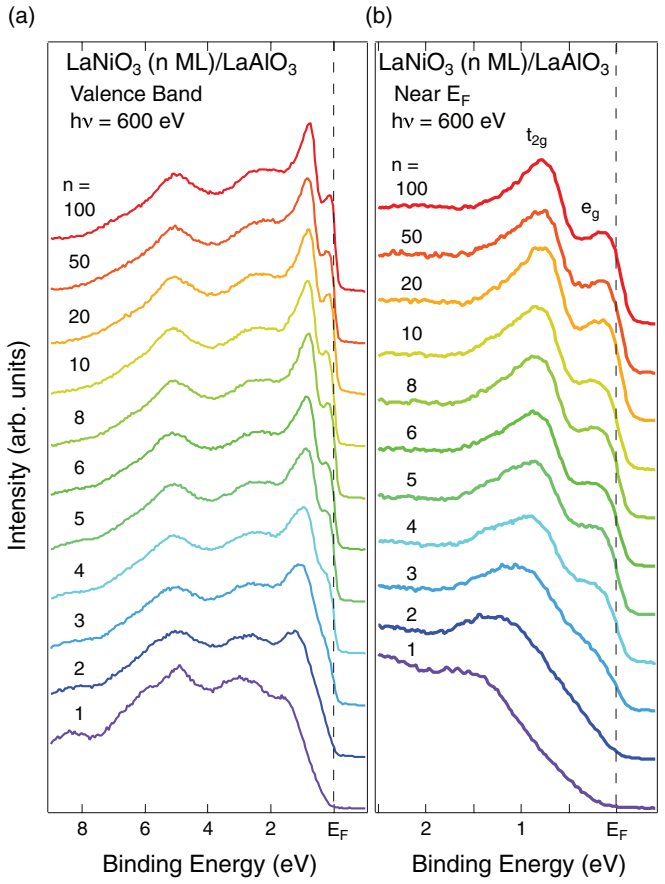

FIG. 2. (Color online) (a) *In situ* valence-band spectra of LNO ultrathin films grown on LAO substrates by digitally controlling the film thickness. (b) PES spectra near E_F.

of an LNO thick film (100 ML). As shown in this figure, atomically flat step-and-terrace structures are observed in the AFM image [Fig. 1(b)], and a chemically abrupt interface is observed in the TEM image [Fig. 1(c)], strongly suggesting that the atomic step-and-terrace structure of a growing LNO film is maintained at the film surface and interface while the film grows to a thickness of hundreds of monolayers. Indeed, almost the same atomically flat step-and-terrace structures reflecting the original surface morphology of LAO substrates were clearly observed in all the measured ultrathin films as partially shown in the inset of Fig. 1(a). This strongly suggests that *in situ* post-annealing process does not deteriorate the film surface. In addition, the TEM measurement confirmed the coherent growth of LNO onto LAO substrates without the formation of any dislocations in LNO films. The sharp XRD patterns with well-defined Laue fringes are clearly observed around the (002) diffraction peaks [Fig. 1(d)], which also indicate the high quality of the present films, as well as the smooth and homogeneously coherent films. These characterization results indicate that there are no detectable structural disorders in LNO ultrathin films grown on LAO, and systematic control of the dimensionality while the fundamental crystallographic parameters of LNO films are fixed has been conducted.

Figure 2(a) shows the valence-band spectra of LNO ultrathin films grown onto LAO substrates by digitally controlling the LNO layer thickness. Since the LAO substrate has a wide band gap of 5.6 eV, the electronic structure near the Fermi level of LNO films is not influenced by a signal from the substrate even for ultrathin films. In films thicker than 20 ML, the line shapes of these spectra are almost identical to each other. The valence-band spectra consist of two structures: two sharp structures derived from Ni e_g and t_{2g} states located at E_F and 0.8 eV, respectively, and broad O-2p derived structures with a binding energy of 2–7 eV.[21] It should be noted that such a sharp two-peak structure of Ni 3d states near E_F has only been observed in a previous *in situ* PES measurement on a LNO thick film having an atomically flat surface[21] and a bulk sensitive hard x-ray PES measurement on a LNO film grown on LAO substrates;[23] this attests to the high quality of the surfaces of the LNO ultrathin films measured in the present study.

When the film thickness is decreased to below 10 ML, the valence-band spectra show remarkable and systematic changes mainly at Ni 3d states near E_F. To investigate the changes in Ni 3d states in more detail, we present the near-E_F spectra according to an enlarged binding energy scale in Fig. 2(b). For film thicknesses of 3–10 ML, the intensity of the Ni-3d-derived peak at E_F gradually decreases, and simultaneously the t_{2g} peak broadens. The leading edge of the Ni 3d states appears to shift from above E_F to below E_F at 3–6 ML, suggesting the evolution of a pseudogap at E_F. With further decreasing film thickness, the density of states (DOS) at E_F becomes negligible, and finally a clear energy gap opens at 1–2 ML. An extrapolation of the linear portion of the leading edge to the energy axis yields a valence-band maxima of 200 meV for a 1-ML film and almost 0 meV for a 2-ML film. The negligibly small residual DOS at E_F for the 2-ML film may be due to the finite energy resolution of our experimental system (120 meV). These results indicate the occurrence of MIT at a critical thickness of 2–3 ML.

The observed spectral behaviors are in line with the results of transport measurements, as shown in Fig. 3. As can be seen in Fig. 3(a), the resistivity versus temperature (ρ-T) curves exhibit dramatic changes as a function of film thickness. The thickness-dependent ρ-T behavior of the LNO ultrathin films can be categorized into three regimes: a metallic regime above 10 ML, an intermediate weakly localized regime of 5–10 ML, and an insulating (strongly localized) regime below 4 ML. The observed ρ-T behaviors in the present study are similar to those in a previous study on a single LNO ultrathin film and LNO-based heterostructures irrespective of the difference in substrates and heterostructures,[4–8] suggesting that the thickness-dependent MIT through an intermediate state is a common feature in LNO at a thin limit. In the metallic regime, the LNO ultrathin film remains metallic down to the lowest temperature of our apparatus and shows a typical Fermi liquid behavior like bulk LNO,[24] as shown in Fig. 3(b). The Fermi liquid behavior is consistent with the existence of a sharp peak just at E_F in the PES spectra above 10 ML. When the film thickness is decreased to below 8 ML, gradually localized behaviors are observed in the intermediate regime of 5–8 ML: The films exhibit metallic behavior at high temperatures but a small upturn in resistivity below ∼15 K for 8 ML, ∼100 K for 6 ML, and ∼110 K for 5 ML [marked by the triangles in Fig. 3(c)]. The existence of the upturn in the ρ-T curves indicates the

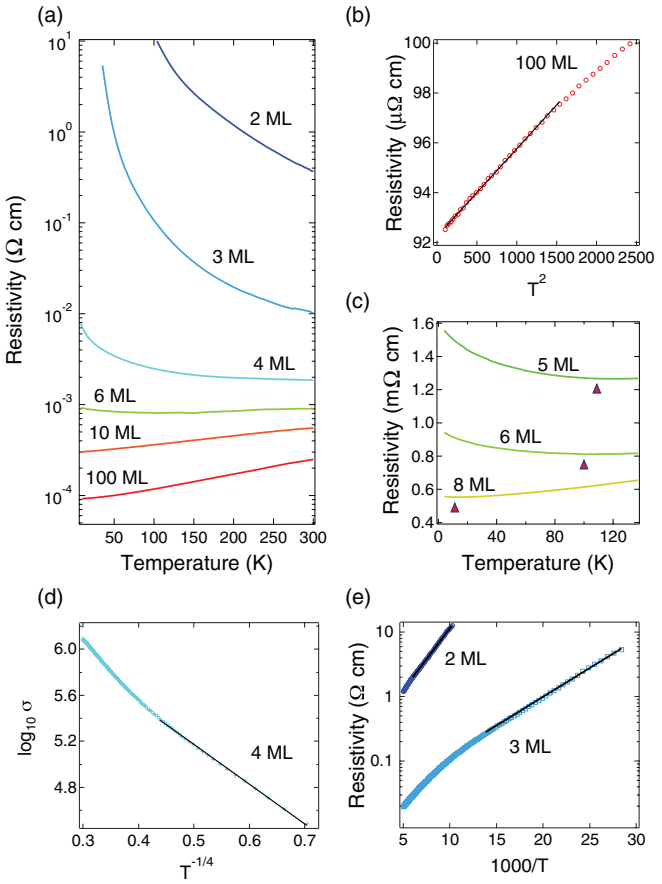

FIG. 3. (Color online) (a) Temperature-dependent resistivity of LNO ultrathin films with variable film thickness. (b) Resistivity data of a 100-ML film plotted against T^2 for temperatures below 50 K. The black line is the linear fit to the data between 10 and 40 K. (c) Resistivity versus temperature for the films in the weakly localized regime. Triangles indicate the local minima of resistivity. (d) Logarithm of conductance (σ) as a function of $1/T^{1/4}$ for a 4-ML film. The black line is the linear fit to the data between 4 and 30 K. (e) Resistivity as a function of $1000/T$ for insulating 2- and 3-ML films. The black lines are the linear fit to the data between 100 and 170 K for a 2-ML film and 35 and 70 K for a 3-ML film.

appearance of weakly localized states in the intermediate regime.

Below 4 ML, the resistivities of the ultrathin films monotonically increase over the entire temperature range with increasing temperature, indicating that strong localization effects are dominant in this regime. For a 4-ML film, a VRH-type behavior is observed [Fig. 3(d)], and for films with thicknesses of 3 and 2 ML, the resistivity is thermally activated down to ∼40 and ∼100 K, respectively. Below these temperatures, the resistivity of ultrathin films becomes so large that constant-current techniques of measurement do not work because of the impedance limitation of our voltmeter. The transport activation energies in temperature windows of 40–70 K and 100–170 K are estimated to be 170 and 380 meV for 3- and 2-ML films [Fig. 3(e)], respectively. These values are comparable to the formation energy of small polarons in transition metal oxides.[25]

The resistivity data clearly show insulating behavior with an Arrhenius-type temperature dependence in films with thickness below 3 ML, whereas a small but non-negligible DOS at E_F is observed for the 3-ML film in the present PES measurements. This disagreement of the critical thickness between PES and transport measurements may be reconciled by considering the existence of metallic islands spreading in the insulating region for the 3-ML film. To verify the possible "electronic phase separation," a microscopic investigation is necessary.

Both the PES and transport results demonstrate that LNO ultrathin films transform from metal to insulator through an intermediate state. The existence of the intermediate state, which is characterized by the gradual localization of conduction carriers from weak localization (Anderson localization behavior) to strong localization (VRH behavior) in films with thicknesses of 4–10 ML, is considered to be the key factor for understanding the origin of the peculiar insulating state in LNO ultrathin films.[6,8] Since these intermediate states seem to have a close relationship with the formation of a pseudogap observed in the present PES measurements, a more detailed analysis of the pseudogap is required to understand the origin of the MIT.

To clarify the formation of the energy gap and pseudogap, we symmetrized the near-E_F spectra with respect to E_F to remove the effects of the Fermi-Dirac function on the spectra.[13,26] The resultant symmetrized spectra are shown in Fig. 4(a). As expected from Fig. 2(b), the change in the spectra is mainly caused by the suppression of the quasiparticle peak at E_F and subsequent formation of a pseudogap and a gap. For quantitative analysis of the spectral change near E_F, we plot the intensity at E_F as a function of the LNO film thickness, as shown in Fig. 4(b). The intensity at E_F is defined as the integrated intensity in the binding-energy range from −40 to 40 meV. In films thicker than 20 ML, a sharp quasiparticle peak is located just at E_F and remains almost unchanged irrespective of film thickness. In contrast, below 10 ML the intensity of quasiparticle peaks monotonically decreases with film thickness. As a result of the suppression of spectral intensity at E_F, a pseudogap structure is apparently formed at E_F below 4 ML. Finally, the DOS at E_F disappears at a film thickness of 1–2 ML, leading to the formation of an energy gap. These results clearly illustrate that the evolution of the pseudogap and the resultant formation of the energy gap at E_F are responsible for the MIT in LNO ultrathin film through the intermediate localized states.

The critical question is what is the origin of the observed pseudogap and energy gap formation. To gain insight into this, we perform layer DMFT calculations using a realistic two-band Hubbard model for nickelates. In this model, two-fold degenerate e_g orbitals are considered with rotationally invariant Coulomb interactions including intraorbital (interorbital) Coulomb repulsion U (U') and interorbital exchange and pair transfer interactions J, with the condition $U' = U - 2J$. Band parameters are taken from Ref. 3 as $t = 0.6$ and $t' = 0.06$ eV using the notation of Lee *et al.*[27] Impurity problems in the layer DMFT are solved by using the exact diagonalization impurity solver with the Arnoldi algorithm.[28,29] We take temperature $T = 10^{-2}$ eV and retain low-energy states with Boltzmann factors larger than 10^{-6}. Throughout this work,

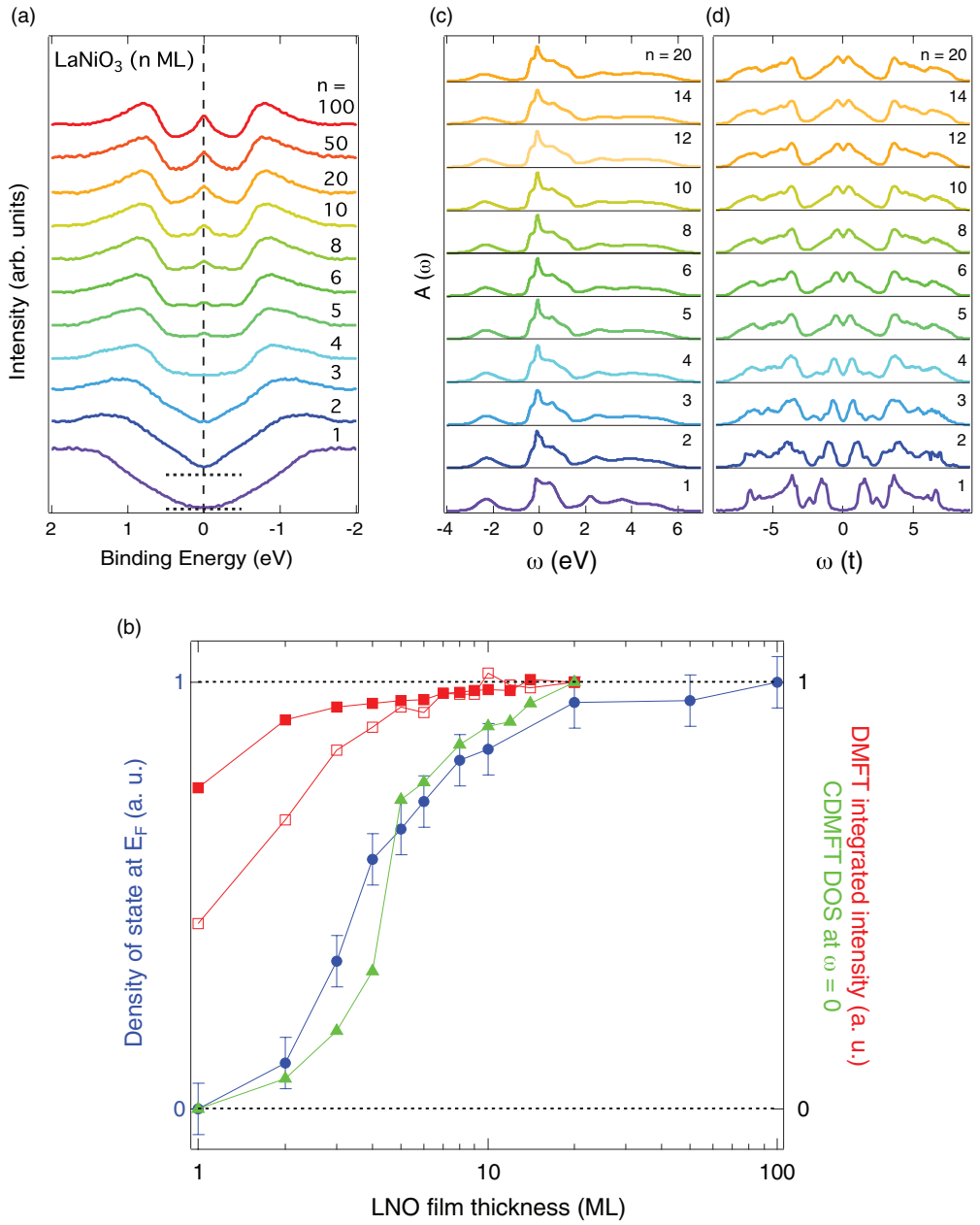

FIG. 4. (Color online) (a) Symmetrized spectra near E_F for thickness-dependent LNO ultrathin films. The dashed lines for 1 and 2 ML indicate the background level. (b) Comparison between the experimental spectral intensity and theoretical ones near E_F as a function of the film thickness. Filled circles are the plots of the DOS near E_F in the symmetrized spectra. Filled (open) squares are the results of layer DMFT with $U = 5$ (7), $J = 0.7$, and $U' = U - 2J$, while filled triangles are the results of layer CDMFT.[6] Experimental results are normalized by the value at $n = 100$, while theoretical results are normalized by the values at $n = 20$. (c) Spectral functions calculated from layer DMFT with $U = 5$, $J = 0.7$ (eV), and $U' = U - 2J$. (d) Those from layer CDMFT with $U/t = 7.5$.

we fix $J = 0.7$ eV (Ref. 3) and only consider paramagnetic states. The spectral function is computed using the self-energy obtained on the real axis, where the delta function is broadened by using the logarithmic Gaussian function.[30] The results for $U = 5$ eV are shown in Fig. 4(c). As subbands cross the Fermi level depending on the film thickness n, the spectral intensity at E_F acquires spurious oscillation. To avoid this, we integrate the spectral intensity from $\omega = -1$ to 0 to compare with the experimental results, as shown in Fig. 4(b). Note that the lower Hubbard bands are located at around 2 eV below E_F, and they should have significant overlap with the fully occupied t_{2g} bands. As expected, the integrated spectral intensity decreases with decreasing n [Figs. 4(b) and 4(c)]. However, the n dependence of the spectral weight is weaker than the experimental observation, and the system remains metallic down to the thinnest system even with a relatively large U. These findings indicate the importance of the factors not accounted for in layer DMFT. The fact that the $n = 1$ system remains metallic even with $U = 7$ eV would mean that the monolayer LNO is not in the strong-coupling Mott regime

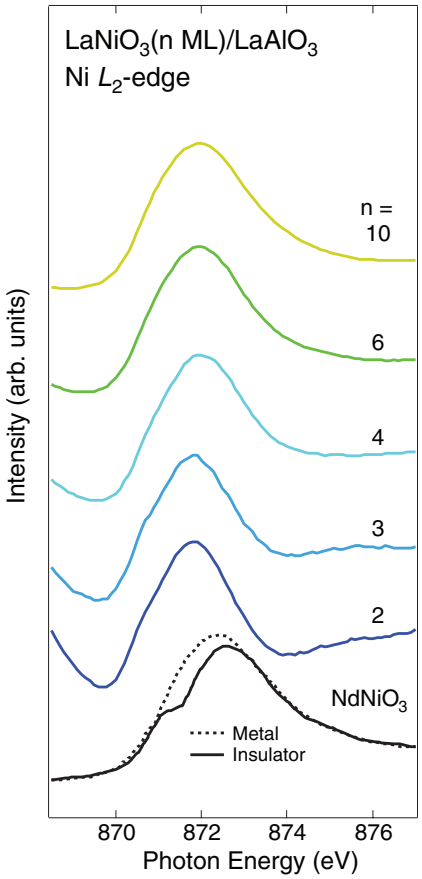

FIG. 5. (Color online) *In situ* XAS spectra at the Ni L_2 edge of LNO ultrathin films on LAO substrates, together with those of a $NdNiO_3$ bulk sample at metallic (dotted line) and insulating (solid line) states (Ref. 33).

but in the intermediate or weak-coupling regime, where spin and/or charge short-range correlation or long-range order is necessary to stabilize insulating states, as discussed by Lee *et al.*[27] In the latter cases, the MIT is expected to become continuous with the pseudogap regime between paramagnetic metallic states and fully gapped insulating states. In fact, the previous layer CDMFT calculations showed a gradual change in the dc conductivity as a function of film thickness[31] accompanied by the opening of the pseudogap.

Let us now compare this feature between the experiment and the theory. In Fig. 4(d) the spectral functions by CDMFT are shown (results for $n \leqslant 6$ are reproduced from Ref. 27), and in Fig. 4(b) the spectral intensity at E_F is plotted as filled triangles. The thickness dependence of low frequency spectral intensity is much closer to the experimental observation. Both theoretical results, layer DMFT and CDMFT, show the gradual change in spectral weight as observed in the PES measurements. A part of this change comes from the change in the bandwidth as captured by the DMFT, yet the experimental results are found to be much closer to the CDMFT results, where the reduction in the spectral intensity accompanies the opening of the pseudogap in accordance with the experiment. This suggests that the observed MIT is due to the crossover from three dimensions to two dimensions during which the in-plane spatial correlation is progressively enhanced. However, the phenomenological CDMFT calculations used a single-orbital Hubbard model where spin correlations are focused. In reality, additional charge correlations and orbital correlations exist. Furthermore, the strong hybridization between Ni 3*d* and O 2*p* orbitals may play important roles at the insulating state and in the critical regime.[32] Incorporating these effects with spatial correlations beyond single-site DMFT formalisms might be necessary to fully understand the nature of MIT in LNO ultrathin films, but we anticipate that similar pseudogap behavior will emerge from spin-orbital-charge correlations in more realistic models.

Finally, we address a fundamental question as to whether the observed thickness-dependent MIT is accompanied by charge disproportionation as observed in other $RNiO_3$ family members. Charge disproportionation concomitant with resultant structural change has been commonly observed for all the members of $RNiO_3$, except LNO, across the temperature-driven MIT.[17,18] Since the charge disproportionation in bulk $RNiO_3$ modulates the local electronic structure around Ni^{3+} ions, the line shape of elementally selective Ni *L*-edge XAS spectra is very sensitive to the occurrence of the charge disproportionation: The characteristic shoulder structure emerges across the transition from the orthorhombic metallic state to the monoclinic insulating state. Thus, Ni *L*-edge XAS has been used as an indicator of the charge disproportionate ion state in $RNiO_3$.[33–36]

Figure 5 shows *in situ* Ni L_2-edge XAS spectra of LNO ultrathin films with a film thickness around the critical film thickness of the MIT. We focus on the Ni L_2 edge to verify the occurrence of charge disproportionation, since the Ni L_3-edge structure overlaps the La M_4 edge because of the close proximity of the two energy levels.[33,34] The XAS spectra of bulk $NdNiO_3$ for both metallic and insulating states are also shown in Ref. 33. For bulk $NdNiO_3$, a clear additional shoulder structure at ~869 eV, indicative of charge disproportionation, appears across the transition from metallic to insulating state, as observed in the Ni L_2-edge spectra of other bulk $RNiO_3$ members.

The spectral shape of LNO ultrathin films in the metallic regime above 6 ML shows close similarity to that of metallic $NdNiO_3$. In contrast, the spectra of insulating LNO ultrathin films below 3 ML exhibit significant differences from insulating $NdNiO_3$: The characteristic low-energy shoulder structure observed in insulating $NdNiO_3$ is almost absent in the insulating phase of LNO ultrathin films. Although a negligibly weak low-energy shoulder structure reminiscent of charge disproportionation seems to exist, this structure may originate from the structural modulation at the interface and/or surface as a result of the reduction in Ni-O covalency at the surface and/or the interface between the film and substrate.[6,37] Thus, from the XAS measurements on the Ni *L* edge, charge disproportionation as observed in bulk $RNiO_3$ is strongly suppressed in the insulating states of LNO ultrathin films. The suppression of charge disproportionation is plausibly a result of epitaxial strain, since similar suppression of charge disproportionation in epitaxial films has been reported for $NdNiO_3$:[33] In an epitaxial film coherently grown on substrate, the in-plane lattice constant is locked to those of substrates, and consequently such an epitaxial strain effect should hinder a first-order MIT accompanied by a structural change.[38,39]

Although we cannot entirely eliminate the possibility of other spin- and/or charge-ordered states for insulating ground states of LNO ultrathin film via the present experiment, it is reasonable to conclude that the intrinsic insulating ground states in LNO ultrathin films are described as novel insulators where the charge disproportionation has minor contribution.

IV. CONCLUSION

In summary, we performed *in situ* PES and XAS measurements to reveal the origin of the peculiar thickness-dependent MIT in LNO ultrathin films. When the film thickness was decreased below 10 ML, the quasiparticle peak at E_F monotonically decreased and a pseudogap was formed at E_F, which was responsible for the weakly localized state observed in transport measurements. The pseudogap finally evolved into a full gap, confirming the thickness-dependent MIT in LNO ultrathin films. The observed thickness dependence of the spectral intensity at E_F was compared with realistic layer DMFT and phenomenological CDMFT calculations. While the significant quasiparticle renormalization is observed, single-site DMFT does not stabilize a "Mott" insulating state at the thinnest system even with a relatively large U. On the other hand, phenomenological CDMFT captures characteristic behavior of the spectral function as the thickness is varied, opening a pseudogap at $n \sim 3$–6 and the full gap at $n \sim 2$. These results indicate that dimensional crossover from three to two dimensions is the key physics for controlling the thickness-dependent MIT in LNO ultrathin films and for stabilizing an insulating state with short-range correlation or some form of long-range order in a thin limit. The XAS results suggest that the charge-disproportionate state usually observed in other insulating $R\mathrm{NiO_3}$ family members is strongly suppressed in the insulating LNO ultrathin films. These results strongly suggest that a novel insulating state is realized in LNO ultrathin films where the charge disproportionation has a minor contribution to the MIT.

ACKNOWLEDGMENTS

The authors are very grateful to A. Fujimori for useful discussions, Y. Yamasaki, H. Nakao, and Y. Murakami for their support in synchrotron based XRD measurement, and A. Yagishita for support in the experiment at the Photon Factory (PF), KEK. This work was supported by a Grant-in-Aid for Scientific Research (A19684010 and S22224005) from the Japan Society for the Promotion of Science (JSPS) and the JST PRESTO program. K.Y. acknowledges the financial support from JSPS for Young Scientists. S.O. was supported by the US Department of Energy, Office of Basic Energy Sciences, Materials Sciences and Engineering Division. This work was carried out at KEK-PF under the approval of the Program Advisory Committee (Proposal Nos. 2010G515 and 2011S2-003) at the Institute of Materials Structure Science, KEK.

*Author to whom correspondence should be addressed; hiroshi.kumigashira@kek.jp

[1] J. Chaloupka and G. Khaliullin, Phys. Rev. Lett. **100**, 016404 (2008).
[2] P. Hansmann, X. P. Yang, A. Toschi, G. Khaliullin, O. K. Andersen, and K. Held, Phys. Rev. Lett. **103**, 016401 (2009).
[3] P. Hansmann, A. Toschi, X. P. Yang, O. K. Andersen, and K. Held, Phys. Rev. B **82**, 235123 (2010).
[4] J. Son, P. Moetakef, J. M. LeBeau, D. Ouellette, L. Balents, S. J. Allen, and S. Stemmer, Appl. Phys. Lett. **96**, 062114 (2010).
[5] J. Son, J. M. LeBeau, S. J. Allen, and S. Stemmer, Appl. Phys. Lett. **97**, 202109 (2010).
[6] J. Liu, S. Okamoto, M. van Veenendaal, M. Kareev, B. Gray, P. Ryan, J. W. Freeland, and J. Chakhalian, Phys. Rev. B **83**, 161102 (2011); **86**, 079904 (2012).
[7] R. Scherwitzl, P. Zubko, C. Lichtensteiger, and J. M. Triscone, Appl. Phys. Lett. **95**, 222114 (2009).
[8] R. Scherwitzl, S. Gariglio, M. Gabay, P. Zubko, M. Gibert, and J. M. Triscone, Phys. Rev. Lett. **106**, 246403 (2011).
[9] A. V. Boris, Y. Matiks, E. Benckiser, A. Frano, P. Popovich, V. Hinkov, P. Wochner, M. Castro-Colin, E. Detemple, V. K. Malik, C. Bernhard, T. Prokscha, A. Suter, Z. Salman, E. Morenzoni, G. Cristiani, H.-U. Habermeier, and B. Keimer, Science **332**, 937 (2011).
[10] E. Benckiser, M. W. Haverkort, S. Brck, E. Goering, S. Macke, A. Frañó, X. Yang, O. K. Andersen, G. Cristiani, H-U. Habermeier, A. V. Boris, I. Zegkinoglou, P. Wochner, H-J. Kim, V. Hinkov, and B. Keimer, Nat. Mater. **10**, 189 (2011).
[11] A. M. Kaiser, A. X. Gray, G. Conti, J. Son, A. Greer, A. Perona, A. Rattanachata, A. Y. Saw, A. Bostwick, S. Yang, S. H. Yang, E. M. Gullikson, J. B. Kortright, S. Stemmer, and C. S. Fadley, Phys. Rev. Lett. **107**, 116402 (2011).
[12] A. Blanca-Romero and R. Pentcheva, Phys. Rev. B **84**, 195450 (2011).
[13] K. Yoshimatsu, T. Okabe, H. Kumigashira, S. Okamoto, S. Aizaki, A. Fujimori, and M. Oshima, Phys. Rev. Lett. **104**, 147601 (2010).
[14] J. B. Torrance, P. Lacorre, A. I. Nazzal, E. J. Ansaldo, and C. Niedermayer, Phys. Rev. B **45**, 8209 (1992).
[15] S. J. May, J.-W. Kim, J. M. Rondinelli, E. Karapetrova, N. A. Spaldin, A. Bhattacharya, and P. J. Ryan, Phys. Rev. B **82**, 014110 (2010).
[16] J. Chakhalian, J. M. Rondinelli, Jian Liu, B. A. Gray, M. Kareev, E. J. Moon, N. Prasai, J. L. Cohn, M. Varela, I. C. Tung, M. J. Bedzyk, S. G. Altendorf, F. Strigari, B. Dabrowski, L. H. Tjeng, P. J. Ryan, and J. W. Freeland, Phys. Rev. Lett. **107**, 116805 (2011).
[17] J. A. Alonso, J. L. García-Muñoz, M. T. Fernández-Díaz, M. A. G. Aranda, M. J. Martínez-Lope, and M. T. Casais, Phys. Rev. Lett. **82**, 3871 (1999).
[18] J. A. Alonso, M. J. Martínez-Lope, M. T. Casais, J. L. García-Muñoz, and M. T. Fernández-Díaz, Phys. Rev. B **61**, 1756 (2000).
[19] K. Horiba, H. Ohguchi, H. Kumigashira, M. Oshima, K. Ono, N. Nakagawa, M. Lippmaa, M. Kawasaki, and H. Koinuma, Rev. Sci. Instrum. **74**, 3406 (2003).
[20] M. Abbate, G. Zampieri, F. Prado, A. Caneiro, J. M. Gonzalez-Calbet, and M. Vallet-Regi, Phys. Rev. B **65**, 155101 (2002).
[21] K. Horiba, R. Eguchi, M. Taguchi, A. Chainani, A. Kikkawa, Y. Senba, H. Ohashi, and S. Shin, Phys. Rev. B **76**, 155104 (2007).
[22] M. Karrev, S. Prosandeev, B. Gray, J. Liu, P. Ryan, A. Karrev, E. J. Moon, and J. Chakhalian, J. Appl. Phys. **109**, 114303 (2011).

[23] A. X. Gray, A. Janotti, J. Son, J. M. LeBeau, S. Ueda, Y. Yamashita, K. Kobayashi, A. M. Kaiser, R. Sutarto, H. Wadati, G. A. Sawatzky, C. G. Van de Walle, S. Stemmer, and C. S. Fadley, Phys. Rev. B **84**, 075104 (2011).

[24] X. Q. Xu, J. L. Peng, Z. Y. Li, H. L. Ju, and R. L. Greene, Phys. Rev. B **48**, 1112 (1993).

[25] M. Imada, A. Fujimori, and Y. Tokura, Rev. Mod. Phys. **70**, 1039 (1998), and references therein.

[26] A. Kanigel, M. R. Norman, M. Randeria, U. Chatterjee, S. Souma, A. Kaminski, H. M. Fretwell, S. Rosenkranz, M. Shi, T. Sato, T. Takahashi, Z. Z. Li, H. Raffy, K. Kadowaki, D. Hinks, L. Ozyuzer, and J. C. Campuzano, Nat. Phys. **2**, 447 (2006).

[27] S. B. Lee, R. Chen, and L. Balents, Phys. Rev. B **84**, 165119 (2011).

[28] R. B. Lehoucq, D. C. Sorensen, and C. Yang, *ARPACK Users Guide* (Society for Industrial and Applied Mathematics, Philadelphia, 1997).

[29] C. A. Perroni, H. Ishida, and A. Liebsch, Phys. Rev. B **75**, 045125 (2007).

[30] O. Sakai, Y. Shimizu, and T. Kasuya, J. Phys. Soc. Jpn. **58**, 3666 (1989).

[31] G. Kotliar, S. Y. Savrasov, G. Pálsson, and G. Biroli, Phys. Rev. Lett. **87**, 186401 (2001).

[32] M. J. Han, X. Wang, C. A. Marianetti, and A. J. Millis, Phys. Rev. Lett. **107**, 206804 (2011).

[33] J. Liu, M. Kareev, B. Gray, J. W. Kim, P. Ryan, B. Dabrowski, J. W. Freeland, and J. Chakhalian, Appl. Phys. Lett. **96**, 233110 (2010).

[34] J. Liu, M. Kareev, S. Prosandeev, B. Gray, P. Ryan, J. W. Freeland, and J. Chakhalian, Appl. Phys. Lett. **96**, 133111 (2010).

[35] V. Scagnoli, U. Staub, A. M. Mulders, M. Janousch, G. I. Meijer, G. Hammerl, J. M. Tonnerre, and N. Stojic, Phys. Rev. B **73**, 100409 (2006).

[36] C. Piamonteze, F. M. F. de Groot, H. C. N. Tolentino, A. Y. Ramos, N. E. Massa, J. A. Alonso, and M. J. Martínez-Lope, Phys. Rev. B **71**, 020406 (2005).

[37] J. Liu, M. Kareev, D. Meyers, B. Gray, P. Ryan, J. W. Freeland, and J. Chakhalian, Phys. Rev. Lett. **109**, 107402 (2012).

[38] D. Okuyama, M. Nakamura, Y. Wakabayashi, H. Itoh, R. Kumai, H. Yamada, Y. Taguchi, T. Arima, M. Kawasaki, and Y. Tokura, Appl. Phys. Lett. **95**, 152502 (2009).

[39] Y. Ogimoto, M. Nakamura, N. Takubo, H. Tamaru, M. Izumi, and K. Miyano, Phys. Rev. B **71**, 060403 (2005).